Quantifying kinetics of mineralization of carbon dioxide by olivine under moderate conditions

Fei Wang, David Dreisinger, Mark Jarvis, Tony Hitchins, Devy Dyson

PII: S1385-8947(18)32434-3
DOI: https://doi.org/10.1016/j.cej.2018.11.200
Reference: CEJ 20502

To appear in: *Chemical Engineering Journal*

Received Date: 20 September 2018
Revised Date: 23 November 2018
Accepted Date: 26 November 2018

Please cite this article as: F. Wang, D. Dreisinger, M. Jarvis, T. Hitchins, D. Dyson, Quantifying kinetics of mineralization of carbon dioxide by olivine under moderate conditions, *Chemical Engineering Journal* (2018), doi: https://doi.org/10.1016/j.cej.2018.11.200

Quantifying kinetics of mineralization of carbon dioxide by olivine under moderate conditions

Fei Wang[*a], David Dreisinger[a], Mark Jarvis[b], Tony Hitchins[b], Devy Dyson[c]

[a] *Department of Materials Engineering, University of British Columbia, Vancouver, British Columbia, V6T 1Z4 Canada*
[b] *Giga Metals Corporation, 203-700 West Pender Street, Vancouver, British Columbia, V6C 1G8 Canada*
[c] *AuTec Innovative Extractive Solutions Ltd.,323 Alexander Street, Vancouver, British Columbia, V6A 1C4*

Abstract

Global warming mitigation is an urgent issue all over the world and the mineralization for CO_2 sequestration is one of the best methods to permanently store CO_2 gas. The current work has developed a quantified mineralization formula through the systematic investigation of the kinetics of mineralization of a dunite containing high-grade olivine under the chemical reaction control. The effect of the most important CO_2 partial pressure, addition of sodium bicarbonate, specific surface area of the olivine, addition of sodium chloride and reaction temperature can be quantified to the 1.6^{th}, 0.8^{th}, 0.7^{th}, 0.34^{th} power and 47.97 kJ/mol activation energy respectively with a relative error less than ±5%. When there was high addition of sodium bicarbonate, the effect of sodium chloride was not significant. Once the addition of sodium bicarbonate and the CO_2 partial pressure were high enough, the mineralization was always controlled by dissolution of olivine. The following quantified mineralization formula has been developed.

$$\alpha = (1 - (1 - k_0 \times [S]^{0.7} \times [P_{CO2}]^{1.6} \times [NaHCO_3]^{0.8} \times e^{(-Ea \times 1000/RT)} \times t)^3) \times 100\%$$

k_0 is the correction factor, related to the mineralization capability of the material and others. The developed formula and the transformations can be applied to predict the mineralization efficiency, the necessary requirements of reaction time, required sodium bicarbonate and the relationship between the required specific

[*] Corresponding Author
E-mail: fei.wang@alumni.ubc.ca

surface area and CO_2 partial pressure. It can be theoretically suitable for the materials where the majority are olivine and it is necessary to carry out several pre-tests to determine the value of the correction factor (k_0).

Keywords: Quantification formula; kinetics; carbon dioxide mineralization; olivine; shrinking core model; chemical reaction control

1. Introduction

The earth has been reported to be warming particularly in recent decades [1,2] with an increase of annually average temperatures, acidification of oceans [3], receding of glaciers [4–6], and rise of sea levels. Increasingly excessive CO_2 levels in the atmosphere is the result of massive anthropogenic activities and dramatic increase of the human population [1]. One of the methods to sequester CO_2 is by mineralization (or called mineral carbonation) [7]. This is the preferred method to permanently store CO_2 without concerns about long-term monitoring [8–14]. Mineralization transforms the carbon dioxide gas into mineral carbonates, which is the most stable form of carbon [15–18] through the chemical reaction between CO_2 and Mg-/Ca-/Fe(Ⅱ)- silicates or oxides. Fortunately, the mineral silicates suitable for the mineralization are abundant all over the world [11,19,20], especially Mg-silicates, such as olivine.

However, the rate of mineralization for CO_2 sequestration is controlled by slow reaction kinetics [7,21], though it is thermodynamically favourable. Thus far, there is no successful application of an economical mineralization process [16,22]. To make the CO_2 mineralization successfully applied, it is necessary to discover the fundamental theory of how the process proceeds and to predict the mineralization efficiency under specific conditions including particle size (R) of raw materials, temperature (T), CO_2 partial pressure (P_{CO2}), addition of additives (m_1, m_2, ..., m_n), solids content (w), agitation of the system (rpm), and reaction time (t). The ideal formula to predict the efficiency with consideration of comprehensive effects of all factors would be the following:

$$\alpha = F(R, T, P_{CO2}, m_1, m_2, \cdots, m_n, w, rpm, t) \quad (1)$$

Where, α represents the mineralization efficiency and $F(x_1, \cdots, x_n)$ is the comprehensive function of all factors.

In fact, this necessity has been attempted recently by a few researchers [23–25]. There has been progress on the study of mineralization of olivine under the condition of addition of over 0.5 m $NaHCO_3$, but the formula developed only focused on two factors, P_{CO2} and temperature. Keleman and Matter [23] and Gadikota et al. [24] developed the formulas in equation (2) and (3) respectively.

$$\alpha = 1.15 \times 10^{-5} \times \sqrt{P_{CO2}} \times e^{-0.00033 \times (T-185)^2} \times t \quad (2)$$

$$\alpha = 1.03 \times 10^{-5} \times \sqrt{P_{CO2}} \times e^{-0.00033 \times (T-185)^2} \times t \quad (3)$$

Where, the unit of P_{CO2} and T are bar and °C respectively; the unit of t is s.

Ji et al. [25] developed the surface coverage model for the product layer diffusion control during the mineralization of fly ash under the conditions of temperature <70 °C and P_{CO2} < 7 bar. The model is equation (4).

$$\alpha = \alpha_{max} \times [1 - \exp(-k_s k_p t)] \quad (4)$$

Where α_{max} is the carbonation capacity of fly ash, %; k_s is the overall mineralization rate constant, mol/min/m^2; k_p is a constant reflecting the percentage of reactive surface of the fly ash, m^2/mol,

Though it fitted the experimental data well, the constants, k_s and k_p varied under different conditions. It is still difficult to predict the unknown mineralization efficiency under a specific condition and to instruct the industrial application.

In order to develop the complete formula which can quantify the comprehensive effects of various factors, it is necessary to systematically investigate the kinetics of the mineralization process of olivine firstly, prior to the successful application of the technology. The choice of a kinetic model is crucial. Classical shrinking core model (SCM) with constant size of particles is a potentially reasonable choice [26–32], which means the overall particle size of the olivine remains relatively unchanged but the non-reacted olivine core becomes smaller with time. The expressions, equation (5), (6) and (7), show that the process would be mainly controlled by mass transport, chemical reaction and product layer diffusion respectively. These expressions are independent of particle size.

$$t = k_1 \times \alpha \tag{5}$$

$$t = k_2 \times [1 - (1 - \alpha)^{1/3}] \tag{6}$$

$$t = k_3 \times [1 - 2\alpha/3 - (1 - \alpha)^{2/3}] \tag{7}$$

Where, k_1, k_2 and k_3 are the corresponding rate constants for the three control types respectively. The rate constant will change with particle size.

This work is designed to systematically research the kinetics and further to develop a complete formula to quantify the kinetics. As the high CO_2 partial pressure is one of the major obstacles of its application [33], the P_{CO2} in this work focuses on pressures below 41 bar which is considered as a relatively moderate condition.

2. Materials and methods

2.1. Materials

A green dunite sample was supported by Sibelco Europe. This sample has an olivine content of 86% (w/w) followed by an enstatite of 6% by the Quantitative X-ray Diffraction (QXRD) analysis. The chemical composition is shown in Table 1, analyzed by Inductively Coupled Plasma - Optical Emission

Spectrophotometry (ICP-OES) after lithium borate fusion. Based on the mineralization of elemental Mg, Fe and Ca, shown in equation (8), the capacity of this material, m, is 0.5407 g CO_2/g dunite. CO_2 gas in this work was supplied by Praxair, which is 99.9% pure. Furthermore, the additives were considered as $NaHCO_3$ and NaCl, which were regarded as the most classically economically-efficient thus far and provided by Fisher Scientific.

Table 1 Chemical composition of the green dunite.

	MgO	SiO_2	FeO[1]	Al_2O_3	Cr_2O_3	NiO	MnO	CaO
Mass, %	45.5	44.4	10.0	0.2	1.0	0.3	0.1	0.2

[1]: Assumed that all the iron is bivalent Fe(Ⅱ).

$$m = \left(\frac{[Mg]}{24.305} + \frac{[Fe]}{55.845} + \frac{[Ca]}{40.078}\right) \times 44.0098 \quad (8)$$

Where, [Mg], [Fe] and [Ca] are the corresponding bivalent metal content in the raw sample calculated from their oxides, %.

The mineralization tests were performed in a 600 mL stainless steel autoclave (No. 5103) provided by Parr Instrument with a 15 mL sampling kit which can continuously take slurry samples from the autoclave for analysis. The range of temperature and pressure remained ± 2 ℃ and ± 1.6 bar. The precision of the whole tests and analysis maintained at ± 4%.

2.2. Methods

The green dunite was ground by a rod mill and then screened to provide samples with narrow size distribution. The sieve sizes were 500 mesh, 400 mesh, 270 mesh, 200 mesh and 170 mesh. As a result, the particles 0 – 25 μm, 25 – 38 μm, 38 – 53 μm and 53 – 75 μm were collected and used for systematic mineralization tests, including the effects of particle size, temperature, P_{CO2}, concentration of additives, rotation speed and solids content. Particle size distribution and specific surface area were determined by a

laser particle size analysis method (Malvern Mastersizer 2000). Before the mineralization reaction was started, approximately 7 bar carbon dioxide gas was purged into the autoclave to dispel any inert gases and the system was heated for approximately 20 minutes until the operating temperature was achieved. Once the temperature stabilized, the CO_2 pressure was increased to the pre-determined target and the reaction commenced. Every hour, a slurry sample was taken through the sampling kit and the solid-liquid separation was effected by a centrifuge system. The solid was washed by deionized water and analyzed for total carbon content by Leco CS 320.

The mineralization efficiency was calculated based on the change in the carbon content of the solid sample, shown in equations (9 – 13). The progress of carbon mineralization with time was fitted to various models to determine the reaction mechanism.

$$\alpha = \frac{m_2 \times \theta_2 - m_1 \times \theta_1}{m} \times \frac{44.0098}{12.011} \times 100\% \quad (9)$$

$$\theta_2 = \frac{m_{co_2} \times \frac{12.011}{44.0098}}{m_1 + m_{co_2}} \quad (10)$$

$$m_{CO_2} = \alpha \times m \times m_1 \quad (11)$$

$$\theta_2 = \frac{\alpha \times m \times \frac{12.011}{44.0098}}{1 + \alpha \times m} \quad (12)$$

$$\alpha = \frac{\theta_2}{m \times (\frac{12.011}{44.0098} - \theta_2)} \times 100\% \quad (13)$$

Where, θ_1 and θ_2 are the carbon contents before and after mineralization, %; m_1 and m_2 are the solids weights before and after mineralization, g; m_{CO_2} is the mineralized CO_2 gas during the reaction, which resulted in the increase of weight of samples.

Since θ_1 is 0 for the dunite in this work, the carbon content after mineralization can be calculated in equation (10). The sequestered CO_2 can be obtained through the corresponding mineralization efficiency, sample mineralization capacity and the initial sample size, by equation (11). By emerging the equation (11), the equation (10) can be simplified to equation (12) where the θ_2 and α have no relationship with the m_1. Therefore, the mineralization efficiency can be calculated by equation (13) by emerging equations (9) and (12). It is only related to the mineralization capacity and the carbon content after the reaction for the dunite in this work. It is suitable for the mineralization efficiency during the continuous sampling for kinetics research.

The FEI Quanta 650 instrument was used to further analyze the transverse surface of particles of the obtained solids by the scanning electron microscope with an energy dispersive X-ray detector (SEM-EDX) method through measuring the molar ratio of Mg, Fe versus Si.

3. Results and discussion

3.1. Effects of comprehensive effects

Prior to systematic research of the kinetics, comprehensive effects of various factors on the mineralization under the conditions below CO_2 super critical pressure were investigated, including the particle size/specific surface area, temperature, CO_2 partial pressure, the addition of $NaHCO_3$ or NaCl, rotation speed, and solids contents.

Firstly, the effect of particle size on the mineralization efficiency is shown in Fig. 1a under the conditions of 185 °C, $P_{CO_2} = 34\ bar$, 10% solids content, 1 m $NaHCO_3$ + 1 m NaCl and 1200 rpm. It is clear that the particle size had a dramatic impact on the efficiency. The finest particle size sample, 0 – 25 μm, can reach 61% mineralization efficiency in 5 hours. By contrast, the 25 – 38 μm sample can only obtain 51% in 12 hours, followed by 26% and 22% for particle size ranges of 38 – 53 μm and 53 – 75 μm respectively. As shown in Fig. 1b, particle size of P80 or P50 values cannot obviously show the considerable difference. In contrast, the

specific surface area clearly indicates the marked differences among the narrow-sized particles. The specific surface area for the particles sizes, 0 – 25 μm, 25 –38 μm, 38 – 53 μm and 53 – 75 μm, was 1.53, 0.27, 0.12 and 0.08 m^2/g respectively. Comparing the differences of the specific surface area with the considerable effect of the narrow particles on the mineralization efficiency, it is found that it was more possible for the mineralization rate of particles to be limited by its specific surface area.

The temperature showed a more complicated effect, as shown in Fig. 1c. In the beginning, the mineralization efficiency increased dramatically from 17% to 72% when the temperature increased from 120 °C to 175 °C under the conditions of 0 - 25 μm, $P_{CO_2} = 34\ bar$, 10% solids content, 1 m $NaHCO_3$ + 1 m NaCl, 1200 rpm for 5 hours. It is well-known that the increase of the temperature can considerably accelerate the diffusion rate of effective ions and also the chemical reaction rate between the effective ions and the unreacted olivine. However, once the temperature exceeded 175 °C, the efficiency significantly decreased. The reason may be closely related to the applied CO_2 partial pressure and the concentration of bicarbonate ions [32, 34]. At this specific P_{CO2}, the high temperature can decrease the effective concentration of bicarbonate ions [34]. The Gibbs free energy of the reaction between CO_2 gas and olivine also becomes less favourable as the temperature increases to over 175 °C. Therefore, it is important to carefully control the temperature according to the P_{CO2}. At 34 bar of P_{CO2}, a suitable temperature for further study was 175 °C.

The mineralization efficiency was proportional to the CO_2 partial pressure, shown in Fig. 1d. When the P_{CO2} increased from 21 bar to 41 bar, the mineralization efficiency increased markedly from 34% to 76% under the conditions of 0 - 25 μm, 185 °C, 10% solids content, 1 m $NaHCO_3$ + 1 m NaCl, 1200 rpm for 5 hours. Theoretically, it is easier for the mineralization process to provide much higher P_{CO2}. However, the supply of high P_{CO2} is a major cost, along with the reactor equipment required [22,35]. It is reasonable to provide a moderate P_{CO2} to accelerate the mineralization rate and to control the costs.

The additives, both sodium bicarbonate and sodium chloride, can remarkably enhance the mineralization process of olivine, shown in Fig. 1e and 1f respectively. The 2 m addition of sodium bicarbonate and sodium chloride can improve the mineralization efficiency from 14% to 71 % and 35% respectively under the conditions of 0 - 25 μm, 185 °C, $P_{CO_2} = 34\ bar$, 10% solids content, 1200 rpm for 5 hours. As shown in Fig. 1e, there was a slight increase of mineralization efficiency to 19% when 0.32 m sodium bicarbonate was introduced into the system. The efficiency had a logarithmic increase with the further addition of sodium bicarbonate, followed by a plateau after 1.5 m addition at 71%. The addition of sodium chloride from 0.5 m to 2.0 m also showed a logarithmic improvement on the mineralization efficiency as a whole. But unlike the addition of sodium bicarbonate, there was no plateau limiting further improvements in the range of 2.0 m sodium chloride addition. More importantly, the sodium chloride gave a much less positive effect on the mineralization compared to sodium bicarbonate. It is noted that the mineralization efficiency for the addition of 1.0 m $NaHCO_3$ + 1.0 NaCl and only 1.0 m $NaHCO_3$ was 61% and 60% respectively under the same conditions. The further addition of sodium chloride can only contribute to less than 2% efficiency increase at a fixed addition of sodium bicarbonate. The addition of sodium bicarbonate is much more significant than the addition of sodium chloride. It may be unnecessary to add sodium chloride once there was specific addition of sodium bicarbonate.

Fig. 1g and 1h shows the effects of rotation speed and solids content on the mineralization respectively under the conditions of 0 - 25 μm, 185 °C, $P_{CO_2} = 34\ bar$, 1 m $NaHCO_3$ + 1 m NaCl for 5 hours. Both the rotation speed and the solids content showed a limited influence. There was only less than a 2% increase when the rotation speed of the system increased from 500 rpm to 1200 rpm, followed by approximately 5% increase at 1500 rpm. Considering the 4% systematic error, the effect of rotation speed is insignificant. Furthermore, the energy inputted increased by approximately 27 times when the rotation speed increased from 500 rpm to 1500 rpm. According to Fig. 1h, the mineralization efficiency decreased less than 3% when the solids content

increased from 10% to 30%, which is in the range of the systematic error. Therefore, it is considered that there was no obvious effect of solids content in the range of 10% - 30% on the mineralization. This is also good for industrial application as higher % solids will reduce reactor size per unit of solids treated. Thus, it is regarded that there were no effects of rotation speed and solids content in a specific range on the mineralization and there will be no more discussion about the rotation speed and solids contents in the following context.

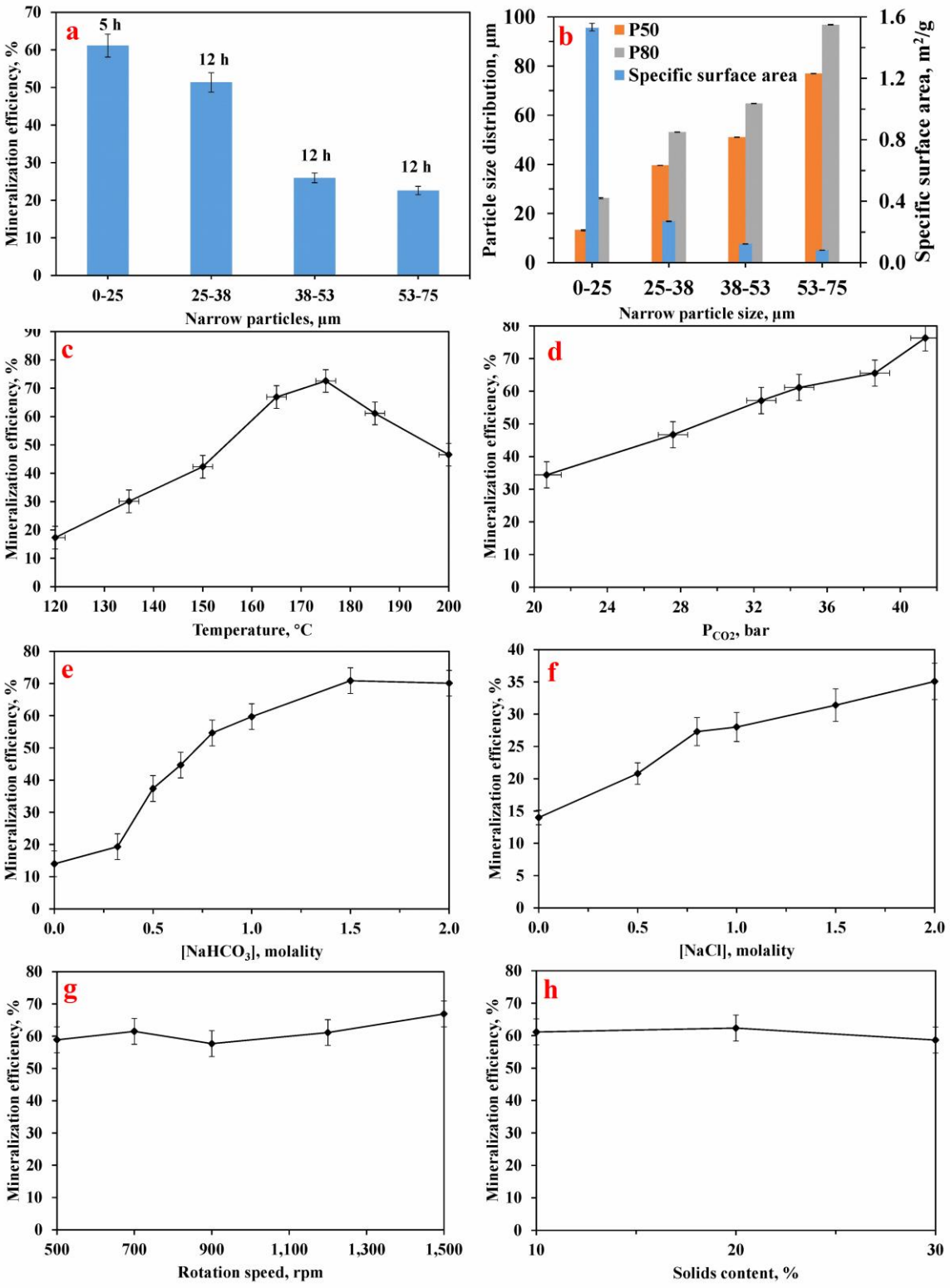

Fig. 1. Comprehensive effects of all factors: (a) Laser particle size distribution and specific surface area of narrow particles; (b) Effect of particle size under 185 °C, $P_{CO_2} = 34\ bar$, 10% solids content, 1 m $NaHCO_3$

+ 1 m NaCl and 1200 rpm; (c) Effect of temperature under 0 - 25 μm, $P_{CO_2} = 34\ bar$, 10% solids content, 1 m $NaHCO_3$ + 1 m NaCl, 1200 rpm for 5 h; (d) Effect of P_{CO2} under 0 - 25 μm, 185 °C, 10% solids content, 1 m $NaHCO_3$ + 1 m NaCl, 1200 rpm for 5 h; (e) Effect of $NaHCO_3$ under 0 - 25 μm, 185 °C, $P_{CO_2} = 34\ bar$, 10% solids content, 1200 rpm for 5 h; (f) Effect of NaCl under 0 - 25 μm, 185 °C, $P_{CO_2} = 34\ bar$, 10% solids content, 1200 rpm for 5 h; (g) Effect of rotation speed under 0 - 25 μm, 185 °C, $P_{CO_2} = 34\ bar$, 10% solids content, 1 m $NaHCO_3$ + 1 m NaCl for 5 h; (h) Effect of solids content under 0 - 25 μm, 185 °C, $P_{CO_2} = 34\ bar$, 1 m $NaHCO_3$ + 1 m NaCl, 1200 rpm for 5 h.

3.2. Kinetics of mineralization

In order to investigate which step controlled the mineralization process, the kinetics was analyzed based on the classical SCM model, shown in Fig. 2. Fig. 2a shows the kinetic plot for narrow particle size sample under the same conditions of under $P_{CO_2} = 34\ bar$, 185 °C content, 1 m $NaHCO_3$ + 1 m NaCl, including mass transport control (Fig. 2a1), chemical reaction control (Fig. 2a2) and product layer diffusion control (Fig. 2a3) respectively. It is obvious that the kinetics of mineralization of all the narrow particle size fractions met the mass transport control or chemical reaction control (R^2 values close to 1). The very fine particles, such as < 5 μm [36], did not obviously affect the kinetics. The sample was prepared using rod-mill grinding. The rod mill prevented the excessive production of ultra-fine particles. For the particle size range of 0 – 25 μm, the particles of less than 5 μm diameters only accounted for 25% of the total mass. It would be difficult for the mineralization process to be controlled by mass transport as the system was very strongly mixed. Given the very slow rate of reaction (partial conversion in +10 h), it is more likely to be controlled by chemical reaction. As the mineralization efficiency decreased when the temperature was over 175 °C, the kinetic data was analyzed only for the temperature below 175 °C (included), shown in Fig. 2b. The kinetic analysis shows that the mineralization at all the temperatures was controlled by mass transport (Fig. 2b1) or

by chemical reaction (Fig. 2b2), rather than by product layer diffusion (Fig. 2b3). In order to further confirm the kinetic control, the mineralized sample under the conditions of 0 – 25 μm, 185 °C, $P_{CO_2} = 34\ bar$, 1 m $NaHCO_3$ + 1 m NaCl, was selected for the SEM-EDX analysis. The images are shown in Fig. 3a. It is clear that the unreacted olivine core was surrounded by crystalline carbonates. The carbonate layer appeared loose and porous. In addition, between the product carbonate layer and the unreacted olivine, there was an empty void. This may be the reason why the mineralization was controlled by chemical reaction and not by the classic shrinking core reaction kinetics. The porous carbonate layer did not form a barrier to diffusion and the void provided a reservoir of aqueous solution with similar concentrations of reactant species to that in the bulk aqueous solution. The activation energy of the reaction will be analyzed to further confirm whether the mineralization was controlled by mass transport or chemical reaction.

The kinetic analysis on the CO_2 partial pressure effect shows a different behaviour, shown in Fig. 2c2. The control of mineralization under the P_{CO2} over 28 bar preferred the chemical reaction. However, when the P_{CO2} was low (lower than 21 bar), the mineralization process was controlled by the product layer diffusion (Fig. 2c3). The corresponding SEM-EDX analysis under the conditions of 0 – 25 μm, 185 °C, $P_{CO_2} = 21\ bar$, 1 m $NaHCO_3$ + 1 m NaCl, is shown in Fig. 3b. It is obviously different compared to Fig. 3a. The crystalline carbonate layer remained present on the outer surface of the unreacted olivine. However, the void found in Fig. 3a was replaced by a dense and poorly porous carbonate layer. The mineralization process was therefore controlled by diffusion through the dense carbonate layer.

The kinetic analysis for the effects of sodium bicarbonate and sodium chloride is shown n Fig. 2d and 2e respectively. When there was no additive, the mineralization process was controlled by product layer diffusion, shown in Fig. 2d3 and 2e3. Even when the addition of additives was low (i.e. less than 0.32 m of sodium bicarbonate), the mineralization was still controlled by diffusion through a product layer. In contrast, it was the chemical reaction that controlled the mineralization process once the usage of additives was more

than 0.32 m, shown in Fig. 2d2 and 2e2. In order to confirm what was the product layer controlling the mineralization, SEM-EDX analysis was used for the sample under the mineralization conditions of 0 – 25 μm, 185 °C, $P_{CO_2} = 34\ bar$ without any additive, shown in Fig. 3c. It is clear that the control mechanism was completely controlled by Si-rich layer diffusion. Compared to Fig. 3c, there was no Si-rich layer in Fig. 3a and 3b. The silica during the mineralization with the addition of 1 m $NaHCO_3$ + 1 m NaCl must have dissolved into the aqueous solution. This may also be the reason why the addition of sodium chloride can markedly enhance the mineralization process. When the addition of additives (sodium bicarbonate or sodium chloride) was low, the silica cannot dissolve into aqueous solution and remained in the product layer, resulting in a poorly porous Si-rich layer. The Si-rich layer prevented the ions from diffusing through the layer to reach the surface of unreacted olivine.

In fact, the mineralization was controlled by product layer diffusion only when the CO_2 partial pressure or the addition of additives was low. Once there was enough addition of additives with more than 21 bar CO_2 partial pressure, the mineralization process was always controlled by chemical reaction. The process controlled by diffusing through product layer is undesirable for industrial applications because of the slow reaction rate. Fortunately, it can be easily addressed through the addition of additives and control of the P_{CO2}. Therefore, only the process controlled by chemical reaction was further considered for the quantification of the kinetics of the effects of factors.

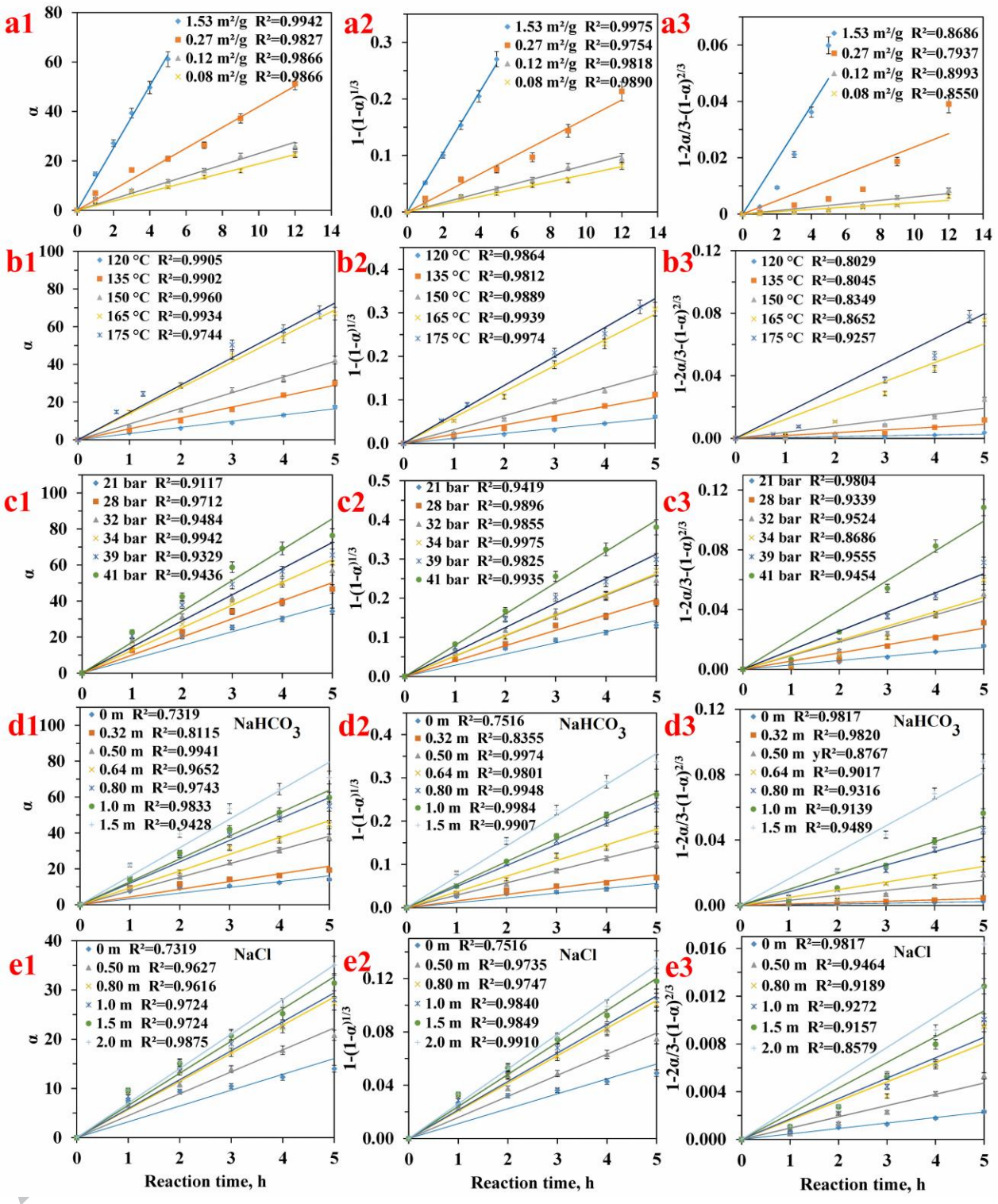

Fig. 2. Plots of kinetics of mass transport control, chemical reaction control and product layer diffusion control respectively: (a) for particle size under $P_{CO_2} = 34\ bar$, 185 °C, 1 m $NaHCO_3$ + 1 m NaCl; (b) for temperature under 0 – 25 μm, $P_{CO_2} = 34\ bar$, 1 m $NaHCO_3$ + 1 m NaCl; (c) for P_{CO2} under 0 – 25 μm,

185 °C, 1 m $NaHCO_3$ + 1 m NaCl; (d) and (e) for $NaHCO_3$ and NaCl respectively under 0 - 25 μm, 185 °C, $P_{CO_2} = 34\ bar$.

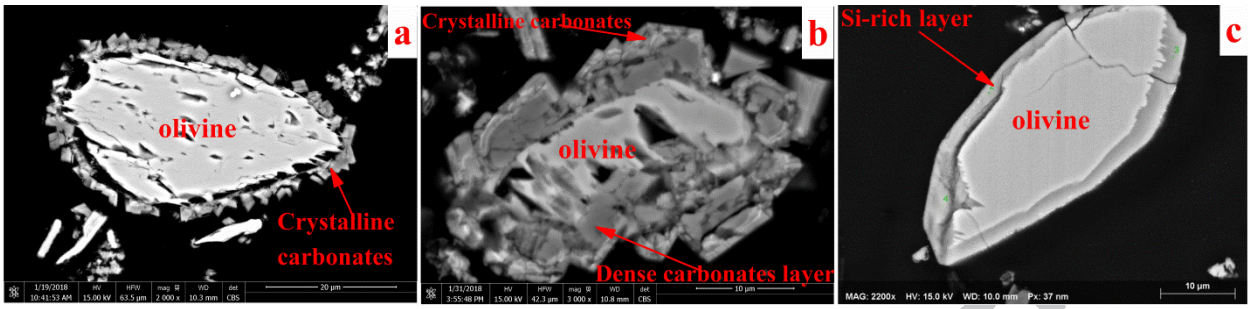

Fig. 3. SEM images of solids after mineralization for: (a) chemical reaction control under 0 – 25 μm, 185 °C, $P_{CO_2} = 34\ bar$, 1 m $NaHCO_3$ + 1 m NaCl; (b) dense carbonates layer diffusion control under 0 – 25 μm, 185 °C, $P_{CO_2} = 21\ bar$, 1 m $NaHCO_3$ + 1 m NaCl; (c) Si-rich layer diffusion control under 0 – 25 μm, 185 °C, $P_{CO_2} = 34\ bar$.

3.3. Quantification of kinetics on effects of factors

Quantifying the factors affecting the kinetics can lead to the development of a formula that is capable of predicting the mineralization efficiency under specific conditions. This can provide significant support for the industrial application and the further development of mineralization technology. This work mainly focused on the mineralization process controlled by the chemical reaction as discussed above. The data from Fig. 2 for quantifying the factors affecting the kinetics are shown in Table 2. In fact, the key to develop the quantification formula is to discover the relationship between the constant k_2 and the factors. As the rotation speed and the solids content had the limited effects on the mineralization, the factors that were taken into consideration were only particle size, temperature, CO_2 partial pressure, and concentration of sodium bicarbonate and sodium chloride. It is more precise and more direct to use the specific surface area other than size of particles because it is the specific surface area that provides the basis for the chemical reaction between the effective ions and the unreacted olivine. The specific surface is not only related to the size of

particles but also the shape and the surface defect of the particles. Therefore, specific surface area was used in place of particle size for the development of the formula.

Table 2 The data for quantifying the factors affecting the kinetics.

Factors		Kinetic control type					
		Mass transport		Chemical reaction		Product layer diffusion	
		k_1	R^2	k_2	R^2	k_3	R^2
Specific surface area, m^2/g	1.53	12.576	0.9942	0.0524	0.9975	0.0096	0.8686
	0.27	4.1923	0.9827	0.0165	0.9754	0.0024	0.7937
	0.12	2.2991	0.9866	0.0083	0.9818	0.0006	0.8993
	0.08	1.8814	0.9866	0.0067	0.9890	0.0004	0.8550
Temperature, °C	120	3.2968	0.9905	0.0115	0.9864	0.0005	0.8029
	135	5.7919	0.9902	0.0212	0.9812	0.0018	0.8045
	150	8.3296	0.9960	0.0318	0.9889	0.0039	0.8349
	165	13.791	0.9934	0.0594	0.9939	0.0121	0.8652
	175	14.512	0.9744	0.0665	0.9974	0.0159	0.9257
CO_2 partial pressure, bar	21	7.6535	0.9117	0.0286	0.9419	0.0029	0.9804
	28	10.035	0.9712	0.0393	0.9896	0.0055	0.0339
	32	12.579	0.9484	0.0518	0.9855	0.0091	0.9524
	34	12.576	0.9942	0.0524	0.9975	0.0096	0.8686
	39	14.497	0.9329	0.0625	0.9825	0.0128	0.9555
	41	17.129	0.9436	0.0798	0.9935	0.0198	0.9454
$NaHCO_3$, m	0	3.2123	0.7319	0.0112	0.7516	0.0005	0.9817
	0.32	4.2978	0.8115	0.0152	0.8355	0.0008	0.9820
	0.50	7.6217	0.9941	0.0286	0.9974	0.0031	0.8767
	0.64	9.3629	0.9652	0.0362	0.9801	0.0048	0.9017
	0.80	11.940	0.9743	0.0487	0.9948	0.0082	0.9316
	1.0	12.764	0.9833	0.0532	0.9984	0.0098	0.9139
	1.5	15.887	0.9428	0.0712	0.9907	0.0162	0.9489
NaCl, m	0	3.2123	0.7319	0.0112	0.7516	0.0005	0.9817
	0.50	4.4556	0.9627	0.0158	0.9735	0.0009	0.9464
	0.80	5.7121	0.9616	0.0207	0.9747	0.0016	0.9189
	1.0	5.8818	0.9724	0.0214	0.9840	0.0017	0.9272
	1.5	6.5391	0.9724	0.0240	0.9849	0.0022	0.9157
	2.0	7.0148	0.9875	0.0261	0.9910	0.0026	0.8579

According to the Arrhenius Equation (equation 14), the constant k in the kinetic model is directly related to the exponential factor A, activation energy and the temperature.

$$k = A \times e^{-Ea \times 1000/RT} \quad (14)$$

Where, k is the rate constant in equation (5 – 7); A is the exponential factor which contains the effects of specific surface area, CO_2 partial pressure, the usage of additives and others; R is the gas constant, 8.314 $J \cdot mol^{-1} \cdot K^{-1}$; T is the temperature, K; Ea is the activation energy of the mineralization process, kJ/mol.

It is important to confirm whether the mineralization process under high addition of additives and over 21 bar CO_2 partial pressure was controlled by chemical reaction. The activation energy combined the above plots of kinetics data and the corresponding SEM-EDX analysis will be used for this purpose. The process which is controlled by chemical reaction usually needs to have an activation energy higher than 40 kJ/mol [26,30]. In order to easily calculate the activation energy, equation 14 can be converted into equation 15, which shows the lnk is linear with 1/T under the specific conditions, shown in Fig. 4a – 4b.

$$lnk = -Ea \times 1000/RT + lnA \tag{15}$$

It is obvious that both lnk_2 and lnk_1 from Table 2 had a good relationship with 1/T, the coefficient was -5.77 and -4.89 respectively. The coefficient is equal to Ea/R. The activation energy was 47.97 kJ/mol and 40.68 kJ/mol with a relative error less than ±2.5% for the chemical reaction control and mass transport control respectively. This analysis confirms that the mineralization process was controlled by chemical reaction rather than by mass transport.

The practical chemical reactions during the mineralization process are the following:

$$4H^+ + Mg_2SiO_4 = 2Mg^{2+} + H_4SiO_{4(a)} \tag{16}$$

$$H_4SiO_{4(a)} = SiO_{2(s)} + 2H_2O_{(l)} \tag{17}$$

$$Mg^{2+} + CO_3^{2-} = MgCO_3 \tag{18}$$

$$HCO_3^- = H^+ + CO_3^{2-} \tag{19}$$

$$H_2CO_{3(a)} = H^+ + HCO_3^- \tag{20}$$

$$CO_{2(a)} + H_2O_{(l)} = H_2CO_{3(a)} \quad (21)$$

$$CO_{2(g)} = CO_{2(a)} \quad (22)$$

Where, reaction (16) is the key to the chemical reaction control. It can be promoted by the increase of the H^+ concentration or the decrease of concentration of the Mg^{2+} and $H_4SiO_{4(a)}$. The aqueous $H_4SiO_{4(a)}$ is not stable and will be decomposed into amorphous silica, shown as reaction (17). If the $H_4SiO_{4(a)}$ decomposes into amorphous silica before it diffuses into the aqueous solution, the amorphous silica will accumulate on the product layer and form the Si-rich product layer (Fig. 3c), which prevents the H^+ from reaching the surface of un-reacted olivine core as shown on the results of mineralization with additives below 0.32 m (included). Once there is sufficient additives in the aqueous solution, the $H_4SiO_{4(a)}$ can rapidly diffuse into the aqueous solution due to the chemical polarity of the high ionic strength solution, followed by a decomposition into amorphous silica in the aqueous matrix, separate from the reacting particle.

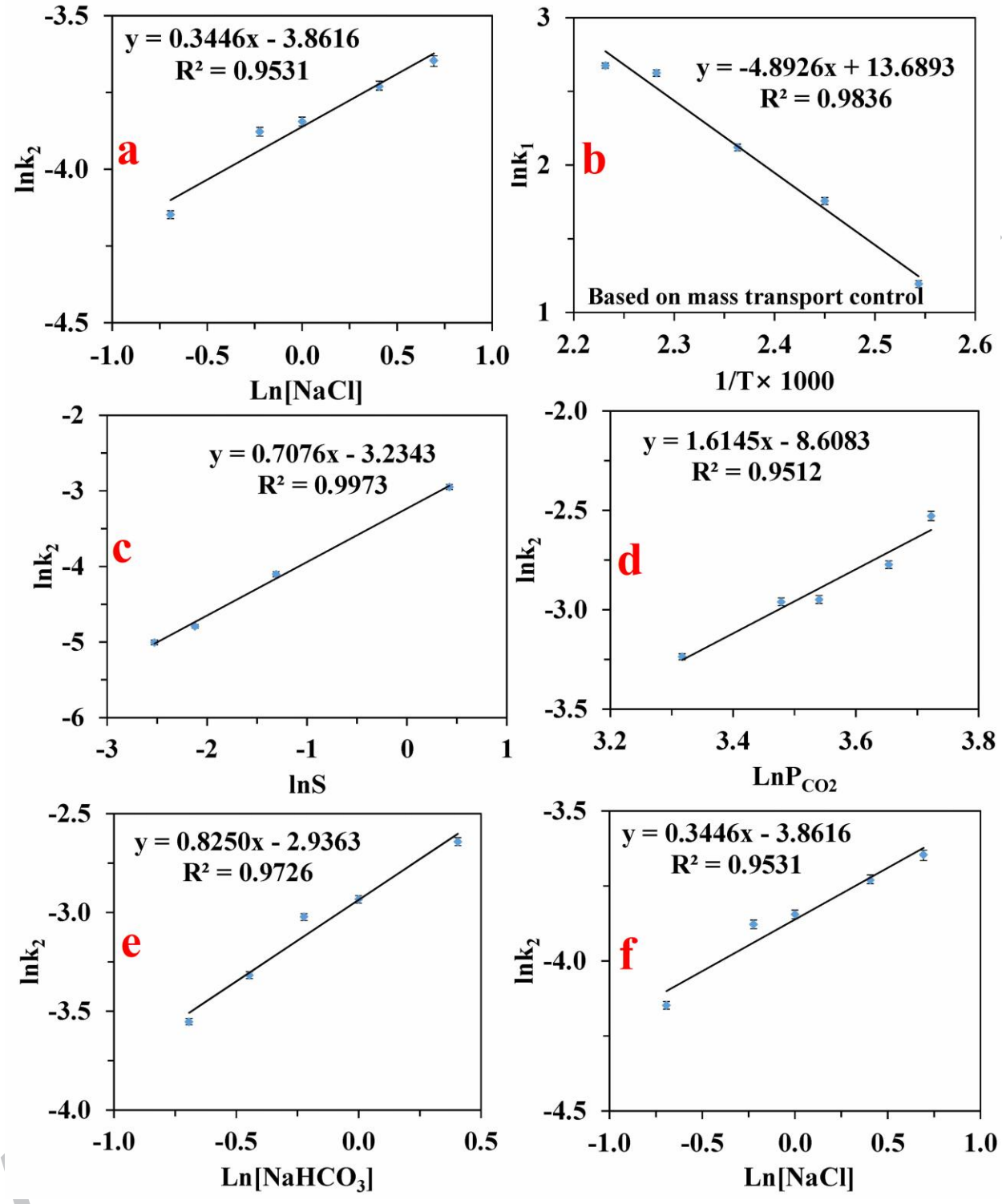

Fig. 4. Quantification of kinetics of effects of factors: (a) activation energy based on chemical reaction control; (b) activation energy based on mass transport control; (c) specific surface area of narrow particles; (d)

CO_2 partial pressure in the mineralization system; (e) addition of sodium bicarbonate and (f) addition of sodium chloride into the mineralization system.

Reaction (18) can decrease the Mg^{2+} concentration further and drive reaction (16) to the right side. The sufficient and instant supply of CO_3^{2-} can ensure the rapid precipitation of $MgCO_3$ as well as the good growth of its crystals as shown on the crystalline carbonates in Fig. 3a. The supply of CO_3^{2-} is mainly from the reaction (19) and (20), the decomposition of HCO_3^- and carbonic acid after a series of chemical reactions (21), and the dissolution of CO_2 gas (22). However, if the CO_3^{2-} is not supplied fast enough, the formation of crystalline carbonates will be limited. By contrast, a dense and poorly porous carbonates layer will be formed as shown in Fig. 3b when the P_{CO2} was below 21 bar, which also prevented the H^+ and Mg^{2+} from diffusing to their targets.

Once the supply of CO_3^{2-} is fast enough and the chemical polarity is high enough, the dissolution of olivine(reaction (16)) controls the mineralization process. The key is the sufficient supply of H^+. It can be dramatically enhanced by the addition of HCO_3^- and the increase of P_{CO2} through reaction (19) and (20) respectively in addition to providing adequate CO_3^{2-}.

Based on the above theory, the addition of $NaHCO_3$ can not only enhance the supply of CO_3^{2-}, but also provide H^+ through the forward and reverse of reaction (19) as well as increase the aqueous ionic strength. It is because of this that the addition of NaCl into the system had the limited effect on the mineralization efficiency once there was enough addition of $NaHCO_3$. The effect of the addition of $NaHCO_3$ was greater than any effect of further addition of NaCl.

Therefore, the effects of NaCl can be neglected once there was addition ($\geq$ 0.5 m) of $NaHCO_3$ during the analysis of quantifying the factors affecting the kinetics. When there was no addition of $NaHCO_3$, the effect of NaCl will be developed separately.

Furthermore, according to equation 15, the lnk is linear with lnA at the specific temperature. The logarithmic value of the constant k_2 listed in Table 2 had been fitted with the logarithmic value of the specific factors, shown in Fig. 4c – 4f. It is clear that the data fit well for all the factors even though some of them had an R^2 value of 0.95.

According to Fig. 4, the order of effects of specific surface area, CO_2 partial pressure and addition of sodium bicarbonate was 0.7, 1.6 and 0.8 also with a relative error ±2.6%, ±4.5% and ±3.5% respectively. The predominant factor was CO_2 partial pressure, approximately twice the order of the effects of the other mainly influential factors. As a result, Formula (23) can be developed. Formula (24) can be derived by combining equation (7) with formula (23). Formula (24) can be further transformed into Formula (25), which shows the calculation of mineralization efficiency under the specific conditions.

$$k_2 = k_0 \times [S]^{0.7} \times [P_{CO2}]^{1.6} \times [NaHCO_3]^{0.8} \times e^{(-Ea\times 1000/RT)} \quad (23)$$

$$1-(1-\alpha)^{1/3} = k_0 \times [S]^{0.7} \times [P_{CO2}]^{1.6} \times [NaHCO_3]^{0.8} \times e^{(-Ea\times 1000/RT)} \times t \quad (24)$$

$$\alpha = (1-(1-k_0 \times [S]^{0.7} \times [P_{CO2}]^{1.6} \times [NaHCO_3]^{0.8} \times e^{(-Ea\times 1000/RT)} \times t)^3) \times 100\% \quad (25)$$

Where, α is mineralization efficiency, %; S is specific surface area of particles, m^2/g; P_{CO2} is CO_2 partial pressure, bar; $NaHCO_3$ is the addition of sodium bicarbonate into the mineralization system, molality; Ea is the activation energy of the mineralization of particles, kJ/mol; R is the gas constant, 8.314 J/(mol·K); T is the system temperature, K; t is the reaction time, h; k_0 is the correction factor.

For all the particles, the correction factor k_0 can be 72 when temperature below 185 °C and be 41 when temperature was 185 °C, shown in Formula (26) and (27) respectively. The Ea can be $47.97 \times (1 \pm 2.5\%)$ kJ/mol according to the above calculation.

$$\alpha = (1-(1-72 \times [S]^{0.7} \times [P_{CO2}]^{1.6} \times [NaHCO_3]^{0.8} \times e^{(-47970/RT)} \times t)^3) \times 100\% \quad (26)$$

$$\alpha = (1-(1-41 \times [S]^{0.7} \times [P_{CO2}]^{1.6} \times [NaHCO_3]^{0.8} \times e^{(-47970/RT)} \times t)^3) \times 100\% \quad (27)$$

According to Formula (26) and (27), the predicted data under all conditions is shown in Fig. 5b – 5f. The predicted data are comparable to the practical data acquired from the tests. The difference is a maximum of only ±5%, which is very close to the range of the precision of the tests, 4%. Therefore, it is suitable for Formula (25) to predict the data under specific conditions.

As to the mineralization without $NaHCO_3$ but only NaCl, Formula (28) can be developed for the mineralization efficiency. The rate constant is proportional to the addition of sodium chloride to the 0.34^{th} power with a relative error ±5.1%.

$$\alpha = (1 - (1 - k_0 \times [S]^{0.7} \times [P_{CO2}]^{1.6} \times [NaCl]^{0.34} \times e^{(-47970/RT)} \times t)^3) \times 100\% \qquad (28)$$

The correction factor k_0 would be 15 at 185 °C, around half of the values of k_0 when $NaHCO_3$ was added. According to Formula (28), the mineralization efficiency can be predicted within a 2% difference as shown in Fig. 5a as long as the process is controlled by reaction (16).

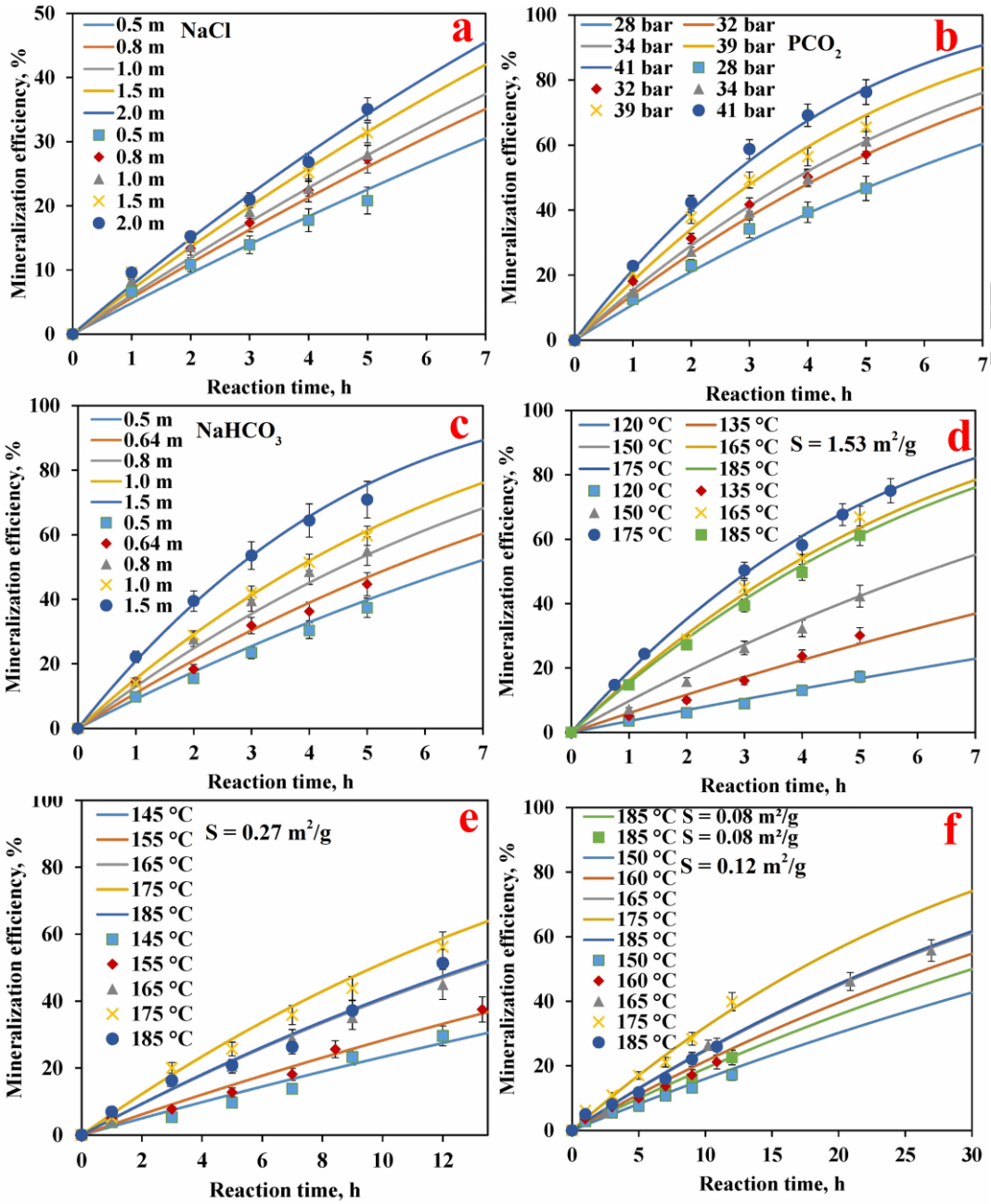

Fig. 5. Prediction of mineralization efficiency according to the developed formulas: (a) for effects of NaCl under 0 – 25 µm, 185 °C, $P_{CO_2} = 34\ bar$; (b) for CO_2 partial pressure under 0 – 25 µm, 185 °C, 1 m $NaHCO_3$; (c) for effects of $NaHCO_3$ under 0 – 25 µm, 185 °C, $P_{CO_2} = 34\ bar$; (d) for system temperature under 0 – 25 µm, $P_{CO_2} = 34\ bar$, 1 m $NaHCO_3$; (e) for system temperature under 25 – 38 µm, $P_{CO_2} = 34\ bar$, 1 m $NaHCO_3$; (f) for temperature under 38 – 53 µm, $P_{CO_2} = 34\ bar$, 1 m $NaHCO_3$ and for 53 – 75

μm with 185 °C under the same conditions. (The solid lines for the prediction data and the shape sign for the practical data from the tests.)

3.4. Application of the quantification formula

As discussed above, the developed quantification formula (Formula 25) can be used to predict the mineralization efficiency according to the listed conditions.

In fact, the quantification can be also used to calculate the time needed to reach the acceptable mineralization efficiency under the specific conditions, shown in Formula 29. For example, it is considered that 80% of the efficiency is acceptable for the mineralization of the particles with 1.53 m^2/g under $P_{CO_2} = 41\ bar$, 175 °C and 1.5 m addition of sodium bicarbonate. According to Formula 29, the required reaction time can be calculated,

$$t \geq (1-(1-\alpha)^{1/3})/(k_0 \times [S]^{0.7} \times [P_{CO2}]^{1.6} \times [NaHCO_3]^{0.8} \times e^{(-Ea\times 1000/RT)}) \quad (29)$$

The experiments showed that the practical time needed for reaction is 4.29 hours, as shown in Fig. 6a, matching with the predicted data very well.

In addition, the formula can also predict the minimum requirement of a specific factor for acceptable mineralization efficiency. For example, Formula 25 can be converted to Formula 30 to predict the requirement of sodium bicarbonate addition. For the particles with 1.53 m^2/g, a mineralization efficiency of 80% under $P_{CO_2} = 41\ bar$, 175 °C for 5.5 hours, then at least 1.1 m sodium bicarbonate addition is required.

$$[NaHCO_3] \geq ((1-(1-\alpha)^{1/3})/(k_0 \times [S]^{0.7} \times [P_{CO2}]^{1.6} \times e^{(-Ea\times 1000/RT)} \times t))^{1/0.8} \quad (30)$$

The practical data shown in Fig. 6b also had a good match with the predicted data through Formula 30.

It is the same way to calculate the requirement of the other factors to reach the specific efficiency under the specific conditions for a specific reaction time.

It is known that the requirements of the specific surface area and the CO_2 partial pressure are the major costs for the application of mineralization for CO_2 sequestration. However, it is difficult to reveal the relationship between the requirements of the minimum specific surface area and CO_2 partial pressure. Fortunately, the quantification Formula 25 can also be transformed into Formula 31 to present the relationship between the required minimum specific surface area and CO_2 partial pressure for specific mineralization efficiency requirement under the specific conditions, as long as the mineralization process is controlled by the chemical reaction.

$$[P_{CO2}] = ((1-(1-\alpha)^{1/3})/(k_0 \times [S]^{0.7} \times [NaHCO_3]^{0.8} \times e^{(-Ea\times 1000/RT)} \times t))^{1/1.6} \quad (31)$$

For any material with a known specific surface area, the minimum specific surface area requirement can be calculated once the other conditions are known as well. According to Formula 31, for instance, for the above dunite, the specific surface area is 1.53 m^2/g, with 80% mineralization efficiency in 5 hours under the conditions of 175 °C and 1.5 m addition of sodium bicarbonate, at least 31 bar of CO_2 partial pressure is needed. The experimental data under the conditions of 31 bar P_{CO2}, 175 °C, 1.5 m sodium bicarbonate and 1.53 m^2/g specific surface area matched the predicted well, as shown in Fig. 6c.

Fig. 6d shows the relationship more clearly between the required P_{CO2} and the specific surface area under the conditions of 175 °C, 1.5 m addition of $NaHCO_3$ for 5 hours. It is assumed that the activation energy Ea and the correction factor k_0 remain at 47.97 kJ/mol and 72 respectively, even though they might need to be corrected slightly. It has been also verified by the samples with S = 0.635, 0.655, 0.941 and 1.53 m^2/g under the P_{CO_2} = 29, 34, 33, 38 and 31 bar to achieve 50%, 60%, 70% and 80% mineralization efficiency respectively. They matched with the predicted well in the range of 1.6 bar for P_{CO2} and 0.08 m^2/g for specific

surface area. Formula 25 and Fig. 6d can be used to support the application of mineralization for CO_2 sequestration.

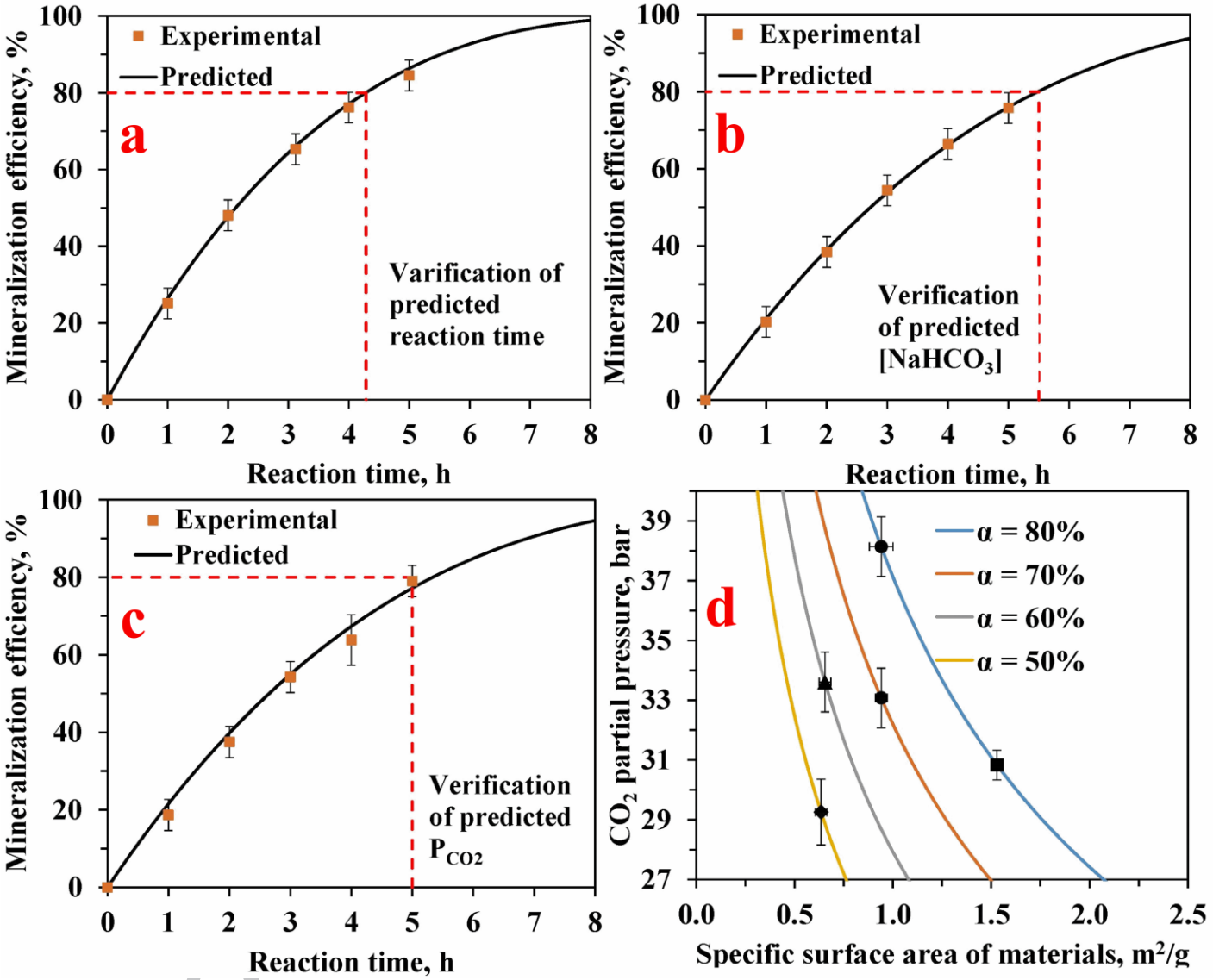

Fig. 6. Application of quantified kinetic formula: (a) verification of predicted reaction time under the conditions of 1.53 m^2/g of specific surface area, $P_{CO_2} = 41\ bar$, 175 °C and 1.5 m addition of sodium bicarbonate; (b) verification of predicted sodium bicarbonate under the conditions of 1.53 m^2/g of specific surface area, $P_{CO_2} = 41\ bar$, 175 °C and 1.1 m addition of sodium bicarbonate; (c) verification of predicted CO_2 partial pressure under the conditions of 1.53 m^2/g of specific surface area, $P_{CO_2} = 31\ bar$, 175 °C and

1.5 m addition of sodium bicarbonate; (d) relationship between specific surface area of materials and the required minimum CO_2 partial pressure to reach the specific mineralization efficiency under the conditions of 175 °C, 1.5 m addition of $NaHCO_3$ for 5 hours (assumed that the activation energy and correction coefficient remained 47.97 kJ/mol and 72 respectively) where the shapes ♦, ▲, ● and ■ represented the experimental data for the samples with 0.635, 0.655, 0.941 and 1.53 m^2/g specific surface area respectively.

Herein, Formula 25 was only developed from the high grade olivine under the chemical reaction control. It can provide the suitable guidelines for the application of mineralization technology. Theoretically, the developed Formula 25 can be also used for any materials where the olivine is the major mineral. However, this must be confirmed by investigating other sources of olivine for comparison. The k_0 value may need to be re-determined through several pre-tests because it is related to the capability of CO_2 sequestration of materials and others.

4. Conclusions

In this paper, comprehensive effects of factors on the mineralization efficiency have been investigated under moderate conditions. The specific surface area, temperature, CO_2 partial pressure and additions of sodium bicarbonate and sodium chloride had considerable effects. The addition of sodium bicarbonate can cover the effects of sodium chloride under certain conditions.

A systematic kinetics analysis has been carried out on the significant factors. It is found that the mineralization process was always controlled by the chemical reaction between protons and the olivine once the addition of sodium bicarbonate and the CO_2 partial pressure were over 0.32 m and 21 bar respectively. The effects of the factors on the reaction kinetics were further quantified through the plotting between the logarithmic value of the rate constant of chemical reaction control and the logarithmic value of the factors. The most influential factor was CO_2 partial pressure to the 1.6^{th} power with a relative error ±4.5%. The

specific surface area of the particles and addition of sodium bicarbonate showed similar effects, with the 0.7^{th} and 0.8^{th} power with the relative error ±2.6% and ±3.5% respectively. A reasonable quantification formula of kinetics was finally developed as Formula 19. The correction factor is related to the mineralization capability of the materials and the others. The developed formula can be applied to predict the mineralization efficiency under the specific conditions and also to calculate the necessary requirements of specific factors. The formula can also show the relationship between the required specific surface area of the material and the minimum CO_2 partial pressure. It can be theoretically suitable for materials where the majority of constituents are olivine and it is necessary to carry out several pre-tests to determine the value of the correction factor.

Conflicts of interest

There are no conflicts to declare.

Acknowledgements

The authors thank the Natural Sciences and Engineering Research Council of Canada (NSERC) (CRDPJ 523097 - 17) for the financial support. Special thanks to Sibelco Europe to provide the green dunite. F. W. thanks the Killam Doctoral Scholarship, Four-Year (4-YF) Fellowship and J Keith Brimacombe Memorial Scholarship for the financial support, thanks Dr. Berend Wassink, Dr. Jianming Lu, Mr. Jacob Kabel and Professor Edouard Asselin for the technical support.

References

[1] Intergovernmental Panel on Climate Change (IPCC): Mitigation of climate change, IPCC, Cambridge University Press, Cambridge (2014).

[2] Á. Galán-Martín, C. Pozo Fernández, A. Azapagic, I. Grossmann, N. Mac Dowell and G. Guillén-Gosálbez, *Energy Environ. Sci.* **11** (2017) 572–581.

[3] L. Kwiatkowski and J. C. Orr, *Nat. Clim. Chang.* **8** (2018) 141–145.

[4] J. A. Screen, C. Deser, D. M. Smith, X. Zhang, R. Blackport, P. J. Kushner, T. Oudar, K. E. McCusker and L. Sun, *Nat. Geosci.* **11** (2018) 155–163.

[5] A. A. Bjørk, S. Aagaard, A. Lütt, S. A. Khan, J. E. Box, K. K. Kjeldsen, N. K. Larsen, N. J. Korsgaard, J. Cappelen, W. T. Colgan, H. Machguth, C. S. Andresen, Y. Peings and K. H. Kjær, *Nat. Clim. Chang.* **8** (2018) 48–52.

[6] A. Kääb, S. Leinss, A. Gilbert, Y. Bühler, S. Gascoin, S. G. Evans, P. Bartelt, E. Berthier, F. Brun, W.-A. Chao, D. Farinotti, F. Gimbert, W. Guo, C. Huggel, J. S. Kargel, G. J. Leonard, L. Tian, D. Treichler and T. Yao, *Nat. Geosci.* **11** (2018) 114–120.

[7] W. Seifritz, *Nature* **345** (1990) 486.

[8] J. Sun, M. F. Bertos and S. J. R. Simons, *Energy Environ. Sci.* **1** (2008) 370–377.

[9] A. Sanna, M. Uibu, G. Caramanna, R. Kuusik and M. M. Maroto-Valer, *Chem. Soc. Rev.* **43** (2014) 8049–8080.

[10] L. C. Pasquier, G. Mercier, J. F. Blais, E. Cecchi and S. Kentish, *Environ. Sci. Technol.* **48** (2014) 5163–5170.

[11] J. M. Matter and P. B. Kelemen, *Nat. Geosci.* **2** (2009) 837–841.

[12] F. Xi, S. J. Davis, P. Ciais, D. Crawford-Brown, D. Guan, C. Pade, T. Shi, M. Syddall, J. Lv, L. Ji, L. Bing, J. Wang, W. Wei, K.-H. Yang, B. Lagerblad, I. Galan, C. Andrade, Y. Zhang and Z. Liu, *Nat. Geosci.* **9** (2016) 880–883.

[13] P. Renforth, C. L. Washbourne, J. Taylder and D. A. C. Manning, *Environ. Sci. Technol.* **45** (2011) 2035–2041.

[14] A. Polettini, R. Pomi and A. Stramazzo, *Chem. Eng. J.* **298** (2016) 26–35.

[15] F. J. Doucet, *Scoping study on CO2 mineralization technologies. Report No. CGS-2011-007*, Pretoria, South Africa (2011).

[16] F. Wang, D. B. Dreisinger, M. Jarvis and T. Hitchins, *Can. Metall. Q.* **57** (2018)46–58.

[17] J. Sipilä, S. Teir and R. Zevenhoven, *Carbon dioxide sequestration by mineral carbonation: Literature review update 2005–2007*, (2008) No. VT 2008-1.

[18] S. R. Gislason and E. H. Oelkers, *Science (80).* **344** (2014) 373–374.

[19] R. E. Martinez, S. Weber and K. Bucher, *Chem. Geol.* **367** (2014) 1–12.

[20] Jr. G. E. Brown, D. K. Bird, T. Kendelewicz, K. Maher, W. Mao, N. Johnson, R. J. Rosenbauer, P.G. García Del Real, 2009 *Annual Report to the Global Climate and ENergy Project*, Stanford University, Stanford, CA, United States. (URL: http://www.stanford.edu/~gebjr/).

[21] A. D. Jacobs, PhD thesis, University of British Columbia, Vancouver, BC, Canada (2014).

[22] A. L. Harrison, I. M. Power and G. M. Dipple, *Environ. Sci. Technol.* **47** (2013) 126–134.

[23] P. B. Kelemen and J. Matter, *Proc. Natl. Acad. Sci.* **105** (2008) 17295–17300.

[24] G. Gadikota, J. Matter, P. Kelemen and A.-H. A. Park, *Phys. Chem. Chem. Phys.* **16** (2014) 4679–4693.

[25] L. Ji, H. Yu, B. Yu, R. Zhang, D. French, M. Grigore, X. Wang, Z. Chen and S. Zhao, *Energy & Fuels* **32** (2018) 4569–4578.

[26] M. Gharabaghi, M. Irannajad and A. R. Azadmehr, *Chem. Eng. Res. Des.* **91** (2013) 325–331.

[27] W. K. O'Connor, D. C. Dahlin, G. E. Rush, C. L. Dahlin and W. K. Collins, Proceedings of the 1st National Conference on Carbon Sequestration, Alexandria, VA, United States, (2001) DOE/ARC-2001-027.

[28] F. Wang, Y. Zhang, T. Liu, J. Huang, J. Zhao, G. Zhang and J. Liu, *Int. J. Miner. Process.* **145** (2015) 87–93.

[29] H. Long and D. G. Dixon, *Hydrometallurgy* **73** (2004) 335–349.

[30] F. Habashi, *Kinetics of Metallurgical Processes*, Metallurgy Extractive Publishing, Québec, 2nd edition (1999).

[31] O. Levenspiel, *Chemical Reaction Engineering*, Wiley, New York, 2nd edition (1999).

[32] S.J. Gerdemann, W.K. O'Connor, D.C. Dahlin, L.R. Penner and H. Rush, *Environ. Sci. Technol.* **41** (2007) 2587–2593.

[33] W. K. O'Connor, D. C. Dahlin, G. E. Rush, S. J. Gerdemann, L. R. Penner, D. N. Nilsen, *Aqueous mineral carbonation: Mineral availability, pretreatment, reaction parametrics and process studies*, Albany Research Center, (2005) DOE/ARC-TR-04-002, Albany, OR, United States.

[34] W. J. J. Huijgen, G. Witkamp and R. N. J. Comans, *Chem. Eng. Sci.* **61** (2006) 4242–4251.

[35] M. E. Boot-Handford, J. C. Abanades, E. J. Anthony, M. J. Blunt, S. Brandani, N. Mac Dowell, J. R. Fernández, M.-C. Ferrari, R. Gross, J. P. Hallett, R. S. Haszeldine, P. Heptonstall, A. Lyngfelt, Z. Makuch, E. Mangano, R. T. J. Porter, M. Pourkashanian, G. T. Rochelle, N. Shah, J. G. Yao and P. S. Fennell, *Energy Environ. Sci.* **7 (**2014) 130–189.

[36] G. Gadikota, E.J. Swanson, H. Zhao and A.-H. A. Park, *I&EC Research*, **53**(2014), 6664-6676.

Highlights

1. The kinetics of factors on CO_2 mineralization by olivine has been quantified.

2. A quantified mineralization calculation formula has been developed and verified.

3. The quantified formula can be used to predict CO_2 mineralization efficiency.

4. The formula can be applied to predict the required factors for CO_2 mineralization.

5. Relationship of requirements between P_{CO2} and specific surface area was formulized.